

Mn³⁺ in Trigonal Bipyramidal Coordination: A New Blue Chromophore

Andrew E. Smith,[†] Hiroshi Mizoguchi,[†] Kris Delaney,[‡] Nicola A. Spaldin,[‡] Arthur W. Sleight,[†] and M. A. Subramanian^{*†}

Department of Chemistry, Oregon State University, Corvallis, Oregon 97330-4003, and Materials Department, University of California, Santa Barbara, California 93106

Received September 30, 2009; E-mail: Mas.Subramanian@OregonState.edu

The development of the first known synthetic blue pigment, Egyptian blue (CaCuSi₄O₁₀), is believed to have been patronized by the Egyptian pharaohs, who promoted the advancement of pigment technologies for use in the arts.¹ The subsequent quest for blue pigments has a rich history linked with powerful civilizations, such as the Han Chinese [Han blue (BaCuSi₄O₁₀)] and the Maya [Maya blue (indigo intercalated in magnesium aluminosilicate clays)]. Currently used blue inorganic pigments are cobalt blue (CoAl₂O₄),² ultramarine (Na₇Al₆Si₆O₂₄S₃),³ Prussian blue (Fe₄[Fe(CN)₆]₃),⁴ and azurite [Cu₃(CO₃)₂(OH)₂].⁵ All suffer from environmental and/or durability issues: Cobalt is considered to be highly toxic. Ultramarine and azurite are not stable with respect to heat and acidic conditions. Prussian blue liberates HCN under mild acidic conditions. In addition, the manufacture of ultramarine involves a large amount of SO₂ emission. Hence, the identification of intense blue inorganic pigments that are environmentally benign, earth-abundant, and durable is important but remains a challenge today. We have discovered that a surprisingly intense bright-blue color is obtained when Mn³⁺ is introduced into the trigonal bipyramidal sites of metal oxides. We have demonstrated this behavior by substituting Mn for In in hexagonal YInO₃ and obtaining a blue color over much of the YIn_{1-x}Mn_xO₃ solid-solution range, in spite of the fact that YInO₃ and YMnO₃ are white and black, respectively. We have also shown that a blue color is obtained when Mn³⁺ is introduced into trigonal bipyramidal sites in other layered oxides. We conclude that the blue color is a consequence of both the crystal field splitting associated with the trigonal bipyramidal coordination and the short apical Mn–O bonds. We expect that our results will lead to routes for the development of inexpensive, earth-abundant, environmentally benign, highly stable blue inorganic pigments.

Both YInO₃ and YMnO₃ are known in the common orthorhombic and centric form of the perovskite structure,^{6,7} but they can also be readily prepared in an acentric hexagonal structure (Figure 1) that is not perovskite-related.^{8,9} This hexagonal structure consists of layers of Y³⁺ ions separating layers of corner-shared MO₃ trigonal bipyramids (M = In, Mn). This structure has been of considerable recent interest because it exhibits an unusual form of improper geometric ferroelectricity accompanied by tilting of the MO₃ polyhedra.^{10–12} Such ferroelectricity is compatible with M-site magnetism and therefore allows multiferroic behavior. Two detailed features of isostructural hexagonal YInO₃ and YMnO₃ are important for this work. First, their basal-plane M–O bond lengths are almost equal (2.05 Å for YMnO₃ and 2.1 Å for YInO₃). Second, the apical Mn–O distances in YMnO₃ (1.86 Å) are considerably shorter than those in the basal plane, while in YInO₃, all of the In–O bonds are roughly the same length. The crystal field splitting of the d-orbital energies in trigonal bipyramidal coordination is shown in

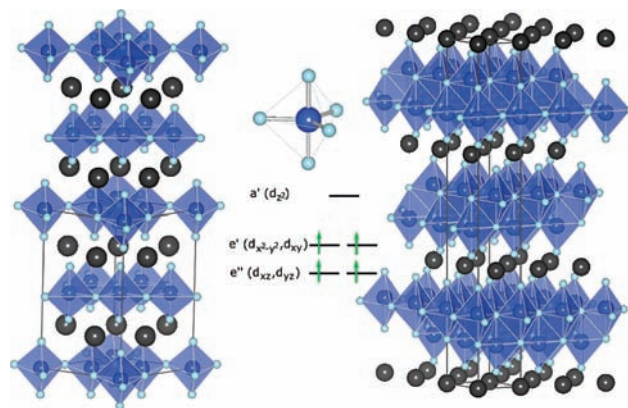


Figure 1. Structures of (left) YMnO₃ and (right) YbFe₂O₄ showing MO₃ trigonal bipyramids in blue (Mn/Fe, blue spheres; O, cyan spheres; Y/Yb, gray spheres). The YMnO₃ structure consists of layers of corner-shared MnO₃ trigonal bipyramids. The YbFe₂O₄ structure is similar but has a double layer of corner-shared FeO₃ trigonal bipyramids that share edges between the layers. Schematic energy levels for the spin-up Mn³⁺ 3d orbitals in trigonal bipyramidal coordination are shown. We note that transitions from e' to a' are formally dipole-allowed in this symmetry

Figure 1. Notably, the e' → a' energy splitting, which is the lowest-energy excitation for a d⁴ cation in the cluster limit, depends sensitively on the apical M–O bond length through its influence on the energy of the d_{z²} orbital. While the crystal field stabilization associated with a d⁴ cation in trigonal bipyramidal coordination has been invoked to explain the stability of hexagonal YMnO₃ relative to the competing perovskite structure, trigonal bipyramidal is not a common coordination for Mn³⁺, and we are not aware of its occurrence in compounds other than hexagonal RMnO₃ compounds in which R is a small rare-earth cation.¹³

In view of the interest in the hexagonal RMnO₃ phases as multiferroic materials, there have been many attempts to substitute Mn with various cations, such as Fe, Co, Ni, Cr, Ti, Ga, and Al.^{14–20} The amount of substitution is always very limited before the structure converts to the perovskite structure, even for those solid-solution compositions where the end-point compound is stable in the hexagonal phase. It is thus surprising that we were able to prepare a complete single-phase YIn_{1-x}Mn_xO₃ solid solution (synthesis details are given in the Supporting Information) despite the fact that the size mismatch between In³⁺ and Mn³⁺ is greater than in the cases where the solid solution is more limited. We attribute this complete miscibility to the similar In–O and Mn–O basal-plane distances in hexagonal YInO₃ and YMnO₃. The large size difference between In³⁺ and Mn³⁺ is manifested only in the apical distances. A plot of unit cell edges for the YIn_{1-x}Mn_xO₃ solid solution is shown in Figure 2. Both the c lattice parameter and the c/a ratio decrease dramatically with x as a result of the short apical Mn–O distances.

[†] Oregon State University.

[‡] University of California, Santa Barbara.

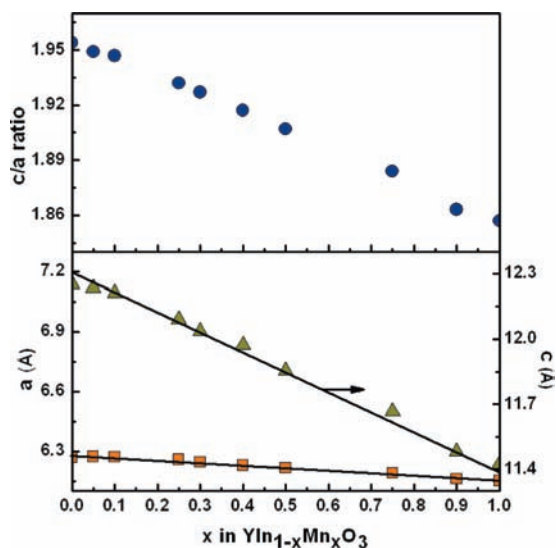


Figure 2. (bottom) Unit cell dimensions a and c and (top) the c/a ratio for the $\text{YIn}_{1-x}\text{Mn}_x\text{O}_3$ solid solution. It is clear that the similar basal-plane bond lengths in the end members lead to a weak variation of a across the solid-solution series. The c/a ratio varies strongly because of the large difference in apical In–O and Mn–O bond lengths.

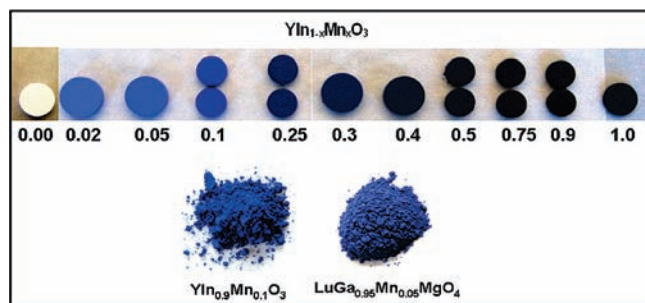


Figure 3. Colors of pellets and powders at selected compositions. The intense blue color appears at our lowest concentration of Mn doping in YInO_3 . With increasing Mn composition, the color darkens until eventually YMnO_3 is found to be black (see the Supporting Information for an enlarged figure).

The blue color of the $\text{YIn}_{1-x}\text{Mn}_x\text{O}_3$ powders is evident even for very low values of x (Figure 3). To understand the origin of this blue color, we measured diffuse reflectance spectra and performed first-principles density functional theory (DFT) calculations with the LSDA+U method, which has been previously shown to give reliable results for YMnO_3 .¹¹ The results of our diffuse reflectance measurements are shown in Figure 4. We see that at low doping concentrations there is a strong, narrow (~ 1 eV width) absorption centered at ~ 2 eV that absorbs in the red-green region of the visible spectrum. The absorption then decreases between 2.5 and 3 eV before a second onset near 3 eV. The absence of absorption in the 2.5–3 eV (blue) region of the spectrum results in the blue color. As the concentration of Mn is increased, the lower-energy absorption peak broadens and the higher-energy onset shifts to lower energy, consistent with the gradual darkening of the samples toward navy blue. In pure YMnO_3 , absorption occurs throughout the entire visible region, resulting in the black color. Although we know of no precedent for a blue color arising from Mn^{3+} in trigonal bipyramidal coordination, a blue color is observed for the d^4 cation Cr^{2+} in trigonal bipyramidal coordination in $[\text{Cr}(\text{Me},\text{tren})\text{Br}]\text{Br}$.²¹ To our knowledge, divalent chromium is not known in oxides.

Our DFT calculations of the densities of states and optical properties of the fully relaxed end-point compounds and selected

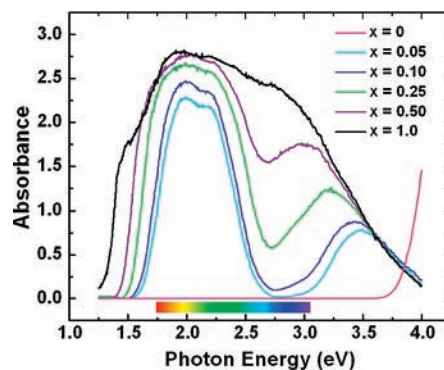


Figure 4. Diffuse reflectance spectra for the $\text{YIn}_{1-x}\text{Mn}_x\text{O}_3$ solid solution. Strong absorption in the red-green spectral region combined with relatively weak absorption in the blue region is responsible for the observed intense blue color. With increasing Mn composition, the first absorption peak broadens and the second onset shifts to lower energy, so YMnO_3 ($x = 1$) absorbs almost equally throughout the visible region (see the text).

intermediates (for details, see the Supporting Information) indicate that the peak at ~ 2 eV arises from the transition between the valence-band maximum, consisting of Mn $3d_{z^2-y^2,xy}$ states strongly hybridized with O $2p_{xy}$ states, and the lowest unoccupied energy level, which in lightly Mn-doped YInO_3 is a narrow band formed from the Mn $3d_{z^2}$ state that lies in the band gap of YInO_3 . (The absence of midgap Mn $3d_{z^2}$ states in pure YInO_3 leaves it colorless). Notably, in the local D_{3h} symmetry of the trigonal bipyramids, the $d-d$ component of this transition (between symmetry labels a' and e'' in Figure 1) is formally symmetry-allowed according to the Laporte selection rule, whereas the $e'' \rightarrow a'$ transition is symmetry-forbidden. This results in a high transition probability and intense absorption. The strong $d-d$ absorption here is in striking contrast to the behavior in the approximate O_h crystal field environment of perovskites, where it is formally symmetry-forbidden. In O_h symmetry, hybridization with ligands or structural distortions are required to circumvent the dipole selection rules, and $d-d$ transitions are usually weak. Indeed, we found no blue color upon substitution of Mn^{3+} into YGaO_3 or YAlO_3 with the perovskite structure, where the Mn^{3+} would be in an environment with approximate O_h symmetry.

We assign the higher-energy peak to the onset of the transition from the O $2p$ band to the Mn $3d_{z^2}$ band. It should be noted that our assignments are consistent with earlier optical studies of YMnO_3 using second-harmonic generation²² but that the topic has been controversial.²³ With increasing Mn concentration, our calculations indicate that the Mn $3d$ levels (particularly the lowest unoccupied state, corresponding to the $3d_{z^2}$ band) broaden substantially, causing the absorption peaks to become broader.

Next we investigated the structural properties of some intermediate compositions in order to determine which structural features correlate with the blue color and in turn to develop guidelines for a general search for blue compounds. Interestingly, our DFT calculations on the relaxed structures for both $\text{Y}_8\text{Mn}_2\text{In}_6\text{O}_{24}$ and $\text{Y}_8\text{Mn}_6\text{In}_2\text{O}_{24}$ units show that while the basal plane Mn–O and In–O distances in these intermediates are similar to each other and to those of the end members, the apical Mn–O and In–O distances are very different from each other, maintaining values close to those of the respective end members (see Table S5 in the Supporting Information). Since the energy of the d_{z^2} state relative to the valence-band maximum is determined primarily by the Mn–O apical bond length, this explains the lack of shift in the energy of the 2 eV absorption peak as a function of Mn concentration. If we artificially insert Mn into the YInO_3 structure without allowing the structure

to relax to its energy minimum, the d_{z^2} peak shifts to considerably lower energy, and the calculated absorption spectrum changes markedly.

For our single-crystal X-ray diffraction study, we focused specifically on the $\text{YIn}_{0.37}\text{Mn}_{0.63}\text{O}_3$ compound and refined the structure using the $P6_3cm$ space group of hexagonal YMnO_3 and YInO_3 . The structure refined normally except for the displacement parameters for one of the apical O atoms, suggesting the presence of static disorder arising from the different In–O and Mn–O distances. Indeed, refinement of the $\text{YIn}_{0.37}\text{Mn}_{0.63}\text{O}_3$ structure with two O atoms at each apical site having occupation values fixed on the basis of the Mn/In ratio converged with shorter distances for the sites with the higher occupation. We extracted apical Mn–O distances of 1.86 and 1.89 Å and apical In–O distances of 2.05 and 2.20 Å, in excellent agreement with the results of our first-principles calculations. Violations of Friedel's law in our diffraction data confirm a polar space group. Relative to the paraelectric structure, displacements of atoms along the c axis, which is the polar axis, are found to be of the same magnitude as in YMnO_3 . However, our first-principles calculations suggest that the polarization might be substantially suppressed from the values in the end-member compounds as a result of frustration of the cooperative tilting by the different sizes of the MO_5 polyhedra. This could lead to intriguing dielectric properties, which will be the subject of future work.

Finally, motivated by our findings in the $\text{YIn}_{1-x}\text{Mn}_x\text{O}_3$ system, we substituted Mn^{3+} into another structure with trigonal bipyramidal sites, the YbFe_2O_4 structure.²⁴ This structure (Figure 1) consists of layers of rare-earth cations alternating with double layers of MO_3 trigonal bipyramids. As in YMnO_3 , the polyhedra in each MO_3 plane share corners through their basal-plane oxygen atoms; here, however, polyhedra in the second plane share edges between apical and basal oxygens with those in the first plane. As in YMnO_3 , the topology of the layering should allow the apical bond lengths to adopt different values for the different M site cations without introducing large strain energies into the lattice. Although YbFe_2O_4 is not a suitable host because of its black color related to $\text{Fe}^{2+}/\text{Fe}^{3+}$ mixed valency, there are several oxides with this structure that are transparent throughout the visible spectrum.²⁵ Again we found that an intense blue color is produced with 5% Mn^{3+} doping into these compounds, which include ScAlMgO_4 , ScGaMgO_4 , LuGaMgO_4 , ScGaZnO_4 , and InGaMgO_4 . Thus, we conclude that the blue color is a general characteristic of Mn^{3+} in a trigonal bipyramidal site in oxides, provided that structural features such as layering allow for the appropriate apical Mn–O bond length.

In summary, we have shown for the first time that an intense bright-blue color occurs through most of the $\text{YIn}_{1-x}\text{Mn}_x\text{O}_3$ solid solution, in spite of the fact that the YInO_3 and YMnO_3 end members are colorless and black, respectively. The compositions as well as color are quite stable under acidic and basic conditions. We have explained the origin of the color through a detailed structural investigation and the use of first-principles DFT calculations. It has been shown that this color is a general feature of Mn^{3+} in trigonal bipyramidal coordination when the structure can accommodate the required short Mn–O apical bonds; this should be particularly favorable in layered structures. Our results suggest

a route to the development of inexpensive, earth-abundant, environmentally benign blue pigments that are based on manganese.²⁶

Acknowledgment. Single-crystal X-ray diffraction data were collected by L. Zakharov, and we thank Alvin Gatimu for help with synthesis. The work at Oregon State University was supported by a grant from NSF (DMR 0804167), and Andrew Smith was supported by an NSF-IGERT grant. N.A.S. and K.D. acknowledge support from NSF under Award DMR-0605852. Calculations were performed at the UCSB California Nanosystems Institute (CNSI) with facilities provided by NSF Award CHE-0321368 and Hewlett-Packard and using TerGrid resources provided by NCSA and supported by NSF.

Supporting Information Available: Details about the synthesis of polycrystalline and single-crystal samples, the X-ray diffraction procedures, and the first-principles calculations; six tables including crystallographic data and structural refinements, bond lengths, anisotropic displacement parameters, distances and polyhedral volumes after relaxation, and first-principles calculations for short apical Mn–O bonds; figures showing sample colors and powder diffraction patterns for all compositions; and crystallographic data (CIF). This material is available free of charge via the Internet at <http://pubs.acs.org>.

References

- (1) Jaksch, H.; Seipel, W.; Weiner, K. L.; ElGoresy, A. *Naturwissenschaften* **1983**, *70*, 525.
- (2) http://en.wikipedia.org/wiki/Cobalt_blue (accessed May 2009).
- (3) <http://en.wikipedia.org/wiki/Ultramarine> (accessed May 2009).
- (4) <http://en.wikipedia.org/wiki/Azurite> (accessed Oct 2009).
- (5) http://en.wikipedia.org/wiki/Prussian_blue (accessed Oct 2009).
- (6) Shannon, R. D. *Inorg. Chem.* **1967**, *6*, 1474.
- (7) Waintal, A.; Chenavas, J. C. R. *Acad. Sci. Paris* **1967**, 264.
- (8) Pistorius, C. W. F. T.; Kruger, J. G. *J. Inorg. Nucl. Chem.* **1976**, *38*, 1471.
- (9) Van Aken, B. B.; Meetsma, A.; Palstra, T. M. *Acta Crystallogr.* **2001**, *C57*, 230.
- (10) Van Aken, B. B.; Palstra, T. M.; Filippetti, A.; Spaldin, N. A. *Nat. Mater.* **2004**, *3*, 164.
- (11) Fennie, C. J.; Rabe, K. M. *Phys. Rev. B* **2005**, *72*, 100103.
- (12) Filippetti, A.; Hill, N. A. *Phys. Rev. B* **2002**, *65*, 195120.
- (13) Yakel, H.; Koehler, W.; Bertaut, E.; Forrat, F. *Acta Crystallogr.* **1963**, *16*, 957.
- (14) Ismailzade, H. I.; Smolenskii, G. A.; Nesterenko, V. I.; Agaev, F. A. *Phys. Status Solidi A* **1971**, *5*, 83.
- (15) Zhou, H. D.; Denyszyn, J. C.; Goodenough, J. B. *Phys. Rev. B* **2005**, *72*, 224401.
- (16) Nugroho, A. A.; Bellido, N.; Adem, U.; Nenert, G.; Simon, C.; Tjia, M. O.; Mostovoy, M.; Palstra, T. T. M. *Phys. Rev. B* **2007**, *75*, 174435.
- (17) Gutiérrez, D.; Peña, O.; Ghanimi, K.; Durán, P.; Moure, C. *J. Phys. Chem. Solids* **2002**, *63*, 1975.
- (18) Peña, O.; Bahout, M.; Gutiérrez, D.; Fernández, J. F.; Durán, P.; Moure, C. *J. Phys. Chem. Solids* **2000**, *61*, 2019.
- (19) Asaka, T.; Nemoto, K.; Kimoto, K.; Arima, T.; Matsui, Y. *Phys. Rev. B* **2005**, *71*, 014114.
- (20) Samal, S. L.; Green, W.; Lofland, S. E.; Ramanujachary, K. V.; Das, D.; Ganguli, A. K. *J. Solid State Chem.* **2008**, *181*, 61.
- (21) Ciampolini, M. *Chem. Commun.* **1966**, 47.
- (22) Degenhardt, C.; Fiebig, M.; Fröhlich, D.; Lottermoser, Th.; Pisarev, R. V. *Appl. Phys. B: Lasers Opt.* **2001**, *73*, 139.
- (23) Kalashnikova, A. M.; Pisarev, R. V. *JETP Lett.* **2003**, *78*, 143.
- (24) Kato, K.; Kawada, I.; Kimizuka, N. *Z. Kristallogr.* **1975**, *141*, 314.
- (25) Kimizuka, N.; Mohri, T. *J. Solid State Chem.* **1985**, *60*, 382.
- (26) There was once in use a blue pigment called Mn-blue. This pigment was prepared from permanganate solutions and has been shown to be BaSO_4 containing Mn^{5+} and Mn^{6+} . The blue chromophore was identified as Mn^{5+} in tetrahedral coordination to oxygen. This pigment is no longer in use because of toxicity issues relating to Ba. The term "Mn-blue" is still used to describe the hue of this Mn-containing pigment (see: Reinen, D.; Brunold, T. C.; Guedel, H. O.; Yordanov, N. D. *Z. Anorg. Allg. Chem.* **1998**, *624*, 438).

JA9080666